JOURNAL OF GEOPHYSICAL RESEARCH, VOL. 112, D05107, doi:10.1029/2006JD007404, 2007

Impacts of land use/cover classification accuracy on regional climate simulations

Jianjun Ge,[1] Jiaguo Qi,[1] Brent M. Lofgren,[2] Nathan Moore,[1]
Nathan Torbick,[1] and Jennifer M. Olson[3,4]

Received 13 April 2006; revised 4 July 2006; accepted 27 August 2006; published 10 March 2007.

[1] Land use/cover change has been recognized as a key component in global change. Various land cover data sets, including historically reconstructed, recently observed, and future projected, have been used in numerous climate modeling studies at regional to global scales. However, little attention has been paid to the effect of land cover classification accuracy on climate simulations, though accuracy assessment has become a routine procedure in land cover production community. In this study, we analyzed the behavior of simulated precipitation in the Regional Atmospheric Modeling System (RAMS) over a range of simulated classification accuracies over a 3 month period. This study found that land cover accuracy under 80% had a strong effect on precipitation especially when the land surface had a greater control of the atmosphere. This effect became stronger as the accuracy decreased. As shown in three follow-on experiments, the effect was further influenced by model parameterizations such as convection schemes and interior nudging, which can mitigate the strength of surface boundary forcings. In reality, land cover accuracy rarely obtains the commonly recommended 85% target. Its effect on climate simulations should therefore be considered, especially when historically reconstructed and future projected land covers are employed.

Citation: Ge, J., J. Qi, B. M. Lofgren, N. Moore, N. Torbick, and J. M. Olson (2007), Impacts of land use/cover classification accuracy on regional climate simulations, *J. Geophys. Res.*, *112*, D05107, doi:10.1029/2006JD007404.

1. Introduction

[2] Human activities are transforming the surface of the Earth at an accelerated pace. Such disturbance of the land can affect local, regional, and global climate by changing the energy balance on the Earth's surface and the chemical composition of the atmosphere [*Chase et al.*, 1999; *Houghton et al.*, 1999; *Pielke*, 2001]. Over the past decades, land use/cover has been widely recognized as a critical factor mediating socioeconomic, political and cultural behavior and global climate change [*International Geosphere-Biosphere Programme* (IGBP), 1990; *Lambin et al.*, 1999; *Watson et al.*, 2000]. Numerous attempts have been made to understand past climate changes and to project potential future climate changes by incorporating reconstructed historical land cover changes and projected possible future land cover changes into numerical simulations [*Xue*, 1997; *Pielke et al.*, 1999; *Chase et al.*, 2000; *DeFries et al.*, 2002; *Taylor et al.*, 2002]. Recent studies have suggested that land use/cover change is a first-order climate effect at the global scale [*Feddema et al.*, 2005].

[3] Until the last decade, land cover products used in most climate models were initially compiled from maps, ground surveys, and various national sources [*Matthews*, 1983; *Olson et al.*, 1983], which have inherent limitations [*Cihlar*, 2000]. In the mid-1990s, global-scale land cover products generated from remote sensing images became available, and have been implemented into various land surface schemes [e.g., *Dickinson et al.*, 1986; *Sellers et al.*, 1986, 1996a, 1996b; *Walko et al.*, 2000]. Recently, more land cover products at regional to global scales have been developed with enhanced qualities, such as Global Land Cover 2000 (GLC2000) and Moderate Resolution Imaging Spectroradiometer (MODIS) land cover [*Mayaux et al.*, 2004; *Friedl et al.*, 2002]. These products have great potential to be employed in numerical modeling systems in the near future.

[4] However, no land cover data set is 100% accurate, even if developed from the most advanced satellite images. Other factors, such as the classification method, the sample size of evaluation data, and the inherent subjective characteristics of classification, can increase the uncertainties contained in land cover data sets. Such limitations have been recognized in the remote sensing community, and therefore quantitative accuracy assessment has been emphasized in most recent land cover classification research [*Foody*, 2002]. Some target accuracy thresholds have recently been recommended in an attempt to provide guide-

[1]Department of Geography and Center for Global Change and Earth Observations, Michigan State University, East Lansing, Michigan, USA.
[2]NOAA/Great Lakes Environmental Research Laboratory, Ann Arbor, Michigan, USA.
[3]Department of Geography, Michigan State University, East Lansing, Michigan, USA.
[4]Also at International Livestock Research Institute, Nairobi, Kenya, Africa.

0148-0227/07/2006JD007404$09.00

Table 1. Percentages and Some Important Biophysical Parameters of the Predominant Five Land Cover Types in GLC2000 After Cross-Referencing[a]

LC Types	Evergreen Broadleaf Forest	Crop/Mixed Farming	Open Shrubland	Grassland	Woodland
Percentages	18.63%	11.66%	11.56%	10.16%	10.12%
Albedo	0.06	0.20	0.12	0.11	0.08
LAI	6.00	6.00	6.00	2.60	5.70
D LAI	1.00	5.50	5.40	2.00	2.30
VFC	0.80	0.85	0.22	0.73	0.80
D VFC	0.10	0.60	0.12	0.11	0.17
Roughness length	2.21	0.06	0.08	0.04	0.83
Root depth	1.20	1.00	0.60	0.70	1.00

[a]LAI and VFC are maximum leaf area index and vegetation fractional cover; D LAI and D VFC are maximum decrease in leaf area index and vegetation fractional cover. These parameters and cosine functions in temperature are utilized for simplified vegetation seasonality. See http://www.atmet.com/html/docs/rams/RT1-leaf2-3.pdf for the more detailed biophysical characteristics of all land cover types defined in LEAF-2.

lines to the classification quality. *Thomlinson et al.* [1999], for example, set as a target an overall accuracy of 85% with no class less than 70% accurate. However, classification accuracy is usually interpreted differently from the viewpoint of various users. The effect of land cover accuracy for a particular application, such as climate modeling in this study, remains an unanswered question. The accuracy targets commonly specified have largely not been tested from the perspective of the operational use of land cover data.

[5] The objective of this paper was to examine how the classification accuracy of a land cover data set employed in a land surface scheme affects simulated cumulative precipitation in a regional climate model. (Here, "regional climate model" means a limited area model with high resolution, generally with grid spacing less than 100 km, run for a simulation time of more than approximately 2 weeks' length, so that the initial atmospheric conditions have been forgotten [*Jacob and Podzun*, 1997].) The hypothesis of this study is that degradation of land cover classification accuracy may not result in a significant change in simulated regional climate until it reaches a certain threshold. By identifying this threshold, the requirement of classification accuracy in regional climate simulation analysis can be determined.

[6] In addition, three follow-on experiments were conducted to investigate how some model parameterizations influence this effect. The parameterizations examined in this study are the convection schemes and interior nudging, which have been shown to influence the atmospheric response to surface boundary forcing [*Weaver et al.*, 2002; *Castro et al.*, 2005]. These follow-on experiments help illustrate how land classification error can propagate to factors that govern precipitation in the model.

2. Methodology

[7] A regional climate model was utilized to simulate the main wet season from March to May for the year 2003 in East Africa. To better represent the land surface characteristics, the default land cover in the model was replaced by a newly developed land cover product from remote sensing images. On the basis of this new land cover, classification error with increasing magnitude was then simulated. Cumulative precipitation from simulations with different classification accuracies was then examined.

2.1. Regional Atmospheric Modeling System

[8] The regional climate model used for the numerical simulations in this work was the Regional Atmospheric Modeling System (RAMS) Version 4.4 [*Pielke et al.*, 1992; *Cotton et al.*, 2003]. RAMS is a three-dimensional, nonhydrostatic, general purpose atmospheric simulation modeling system, which solves equations of motion, heat, moisture, and mass continuity in a terrain-following coordinate system.

[9] RAMS4.4 is an atmospheric model which is capable of both numerical weather prediction and regional climate simulation. In a philosophical sense, numerical weather prediction depends on the initial values of the state variables of the atmosphere. On the other hand, climate simulation is run for longer periods of time, so that it is insensitive to the initial conditions but dependent on boundary conditions such as ocean temperature, land use, and greenhouse gas concentrations [*Giorgi and Mearns*, 1999]. This simulation includes some parts of the climate system such as a full treatment of atmospheric dynamics, thermodynamics and moist processes, along with a Soil-Vegetation-Atmosphere Transfer (SVAT) scheme. However, unlike some climate models it does not include a fully interactive ocean, but treats ocean surface temperature as a prescribed boundary condition.

[10] The SVAT scheme employed in RAMS is the Land Ecosystem-Atmosphere Feedback model, version 2 (LEAF-2) [*Lee*, 1992; *Walko et al.*, 2000]. LEAF-2 represents the storage and vertical exchange of water and energy in multiple soil layers, temporary surface water or snow cover, and vegetation and canopy air. The special feature of LEAF-2 is its ability to represent fine-scale surface variations by dividing surface grid cells into subgrid patches, which are assigned based the land cover types in a model grid cell. Each patch has one land cover type and responds to and influences the overlying atmosphere in its own unique way according to its fractional area of coverage. The biophysical characteristics, such as albedo, leaf area index, fractional vegetation cover, etc., are then defined for the land cover type each patch possesses (See Table 1 and http://www.atmet.com/html/docs/rams/RT1-leaf2-3.pdf for the biophysical characteristics of land cover types defined in LEAF-2). In the experiments presented here, the number of patches per grid cell was set to ten for a relatively detailed representation of the land surface. One patch is allocated for water in all grid cells.

[11] The soil model in LEAF-2 consisted of 11 vertical layers spanning a depth of 2.1 m, and the soil temperature profile in the initial conditions was determined by a deviation from the initial air temperature in the lowest atmospheric

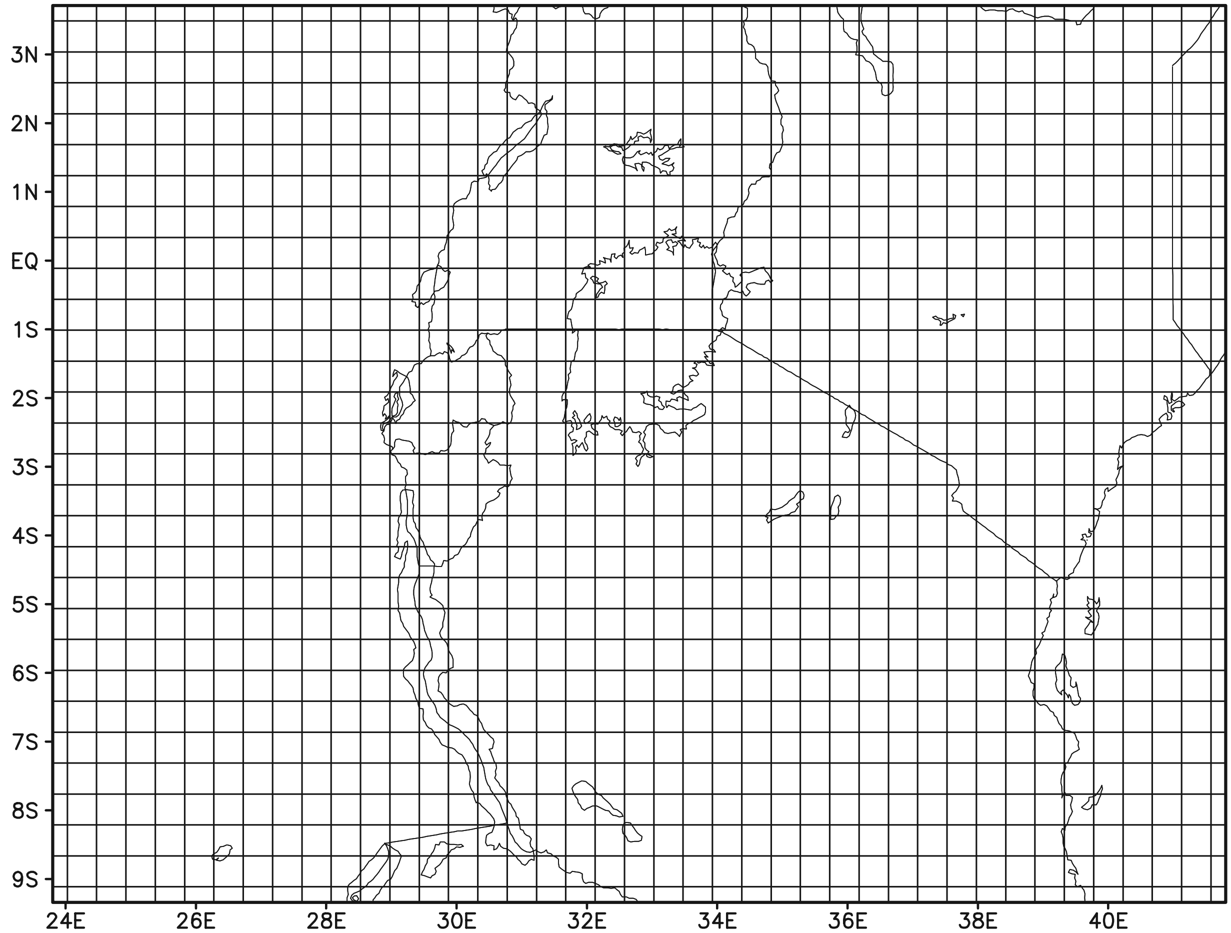

Figure 1. RAMS domain for land cover accuracy examination with Δx = 50 km.

level. The soil moisture content for the top layer was initialized as 35% of the saturation value, which was horizontally homogeneous over the domain. This percentage was increased with depth to a maximum of 55% at 48 cm and below. Moisture flux between soil layers was parameterized in LEAF-2 based on a multilayer soil model described by *Tremback and Kessler* [1985]. Both energy and moisture fluxes between LEAF-2 components (i.e., vegetation, canopy air, and each soil and snow cover layer) are illustrated in detail by *Walko et al.* [2000].

[12] Soil moisture can play an important role in surface-atmosphere interactions particularly through moisture "memory" in semiarid regions like in Kenya and Tanzania (Figures 1 and 2a). The presence of soil moisture influences the partitioning of latent and sensible heat, thereby affecting the development of shallow convection. However, soil types in East Africa are poorly mapped, and available soil moisture values for the region are speculative due to data scarcity. We want to emphasize that the role of surface parameters, including soil moisture, can strongly affect the model solution. In the absence of reliable data, and to avoid introducing more complex uncertainties into this experiment, we chose this homogeneous approach.

[13] A single grid with a 1600 $\times$ 2100 km area was used as the model domain of the experiments, which covers most of East Africa and a small segment of the Indian Ocean (Figures 1 and 2a). The horizontal grid spacing was set at 50 km in consideration of the domain size and the computational requirements. For the land surface, the standard RAMS 30-arc sec topography data set was used. The grid extended over 32 vertical levels, with a layer thickness of 80 m near the surface and stretching to 1900 m at the top of the domain. The model was driven by 6-hourly lateral boundary conditions derived from National Centers for Environmental Prediction (NCEP) atmospheric reanalysis product [*Kalnay et al.*, 1996]. The model time step was 90 s with the output period set to every 6 hours. At each time step, the reanalysis data were nudged over five outer grid points. The months of March, April, and May of 2003 were chosen to simulate because this time period corresponds to the main rainy season across much of this region and the surface effect on precipitation can be analyzed clearly.

[14] The radiative transfer scheme of Chen-Cotton [*Chen and Cotton*, 1983] was used to parameterize the vertical flux of shortwave and longwave radiation. Horizontal diffusion coefficients were computed based on the modified Smagorinsky formulation [*Smagorinsky*, 1963], and the vertical diffusion was parameterized according to the Mellor-Yamada scheme [*Mellor and Yamada*, 1982]. The bulk microphysics parameterization was activated, which allows the model to consider the effect of moisture in all phases. The sea surface temperature was specified using the 1° monthly climatological data set from NCEP [*Reynolds and Smith*, 1994].

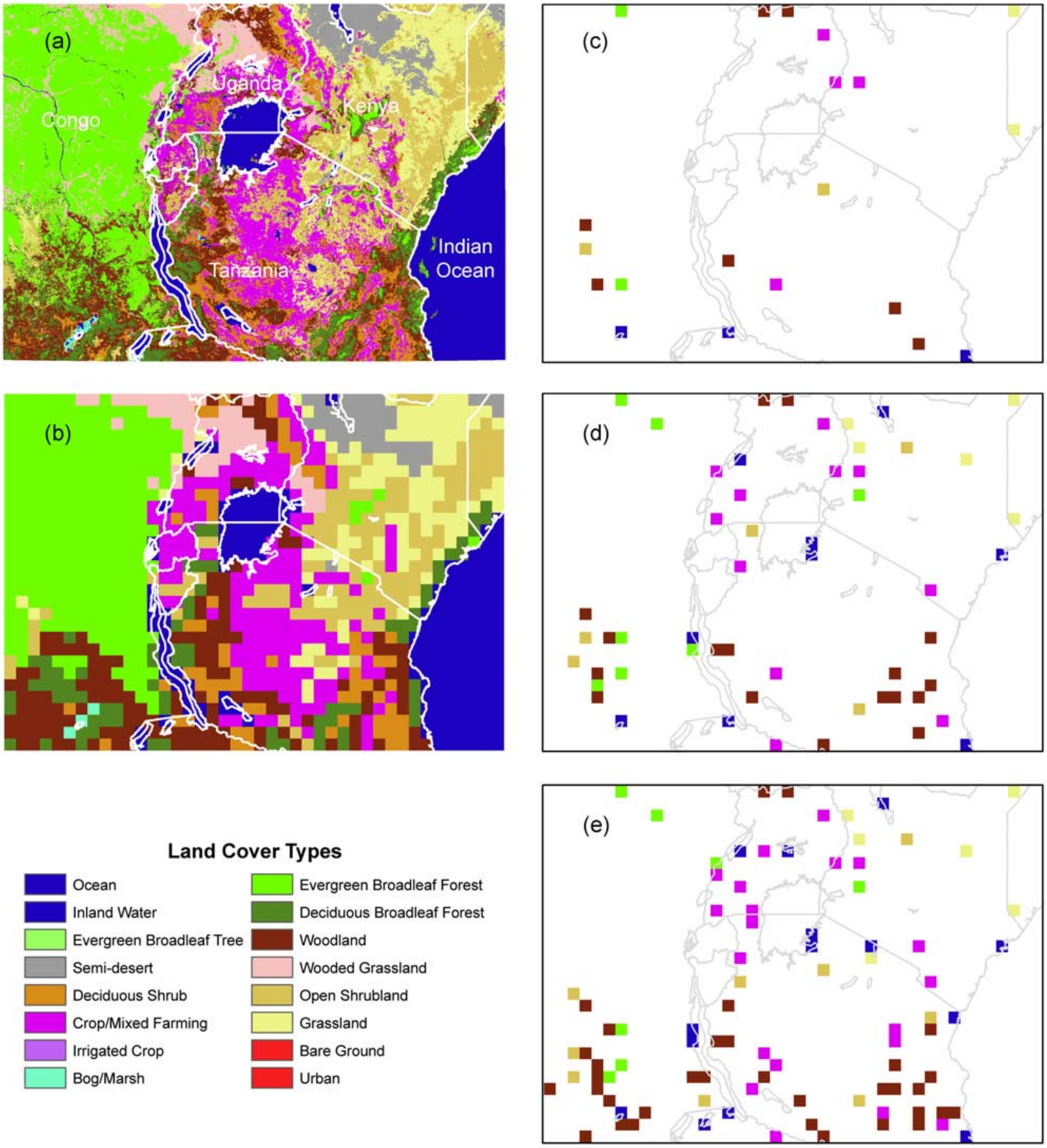

Figure 2. Cross-referenced GLC2000 with (a) 1 km resolution and (b) 50 km resolution, and simulated land cover classification errors: (c) 10%, (d) 30%, and (e) 50%. Land cover types in Figures 2b, 2c, 2d, and 2e only represent the biggest patches in grid cells. See texts for more details.

[15] In the basic experiment, the Kain-Fritsch (KF) convection scheme [*Kain and Fritsch*, 1993] was used with no interior nudging. In the three follow-on experiments, the effects of a different convection scheme [*Kuo*, 1974] and interior nudging were explored.

2.2. Land Cover Data Set

[16] The default land cover used in LEAF-2 is cross-referenced from the Olson Global Ecosystems (OGE) data set with 1 km spatial resolution [*Walko et al.*, 2000]. During the cross-referencing process, similar land categories in OGE are connected to the land surface scheme in LEAF-2 in order to assign relevant biophysical parameters to a given land cover type. OGE was derived from the Global Land Cover Characterization (GLCC) database, which was based primarily on 1 km advanced very high resolution radiometer (AVHRR) data spanning from April 1992 through March 1993 [*Loveland et al.*, 2000]. GLCC was one of the earliest

global land cover data sets derived primarily from remote sensing images, and it was an improvement over former data sets compiled from maps and survey data. It was thus widely used in various land surface schemes in climate models and other scientific research such as agricultural production modeling [*Brown et al.*, 1999].

[17] However, new global land cover products, such as GLC2000, have advantages over GLCC. They were developed from satellite images with enhanced spectral, spatial, radiometric, and geometric quality. More importantly, land surface conditions in this region have been substantially changed by human activities during the past decade due to increased population and other factors. Therefore the OGE data set was replaced in this study by a newer land cover product to better represent the land surface. Several global and regional products were evaluated based on a newly developed statistical method. GLC2000 for Africa was found to be the most accurate for this region [*Ge et al.*, 2007]. GLC2000 was developed by the Joint Research Centre's Global Vegetation Unit, based primarily on SPOT VEGETATION daily 1 km data acquired from 1 November 1999 to 31 December 2000 [*Mayaux et al.*, 2004]. It uses the Land Cover Classification System [*Di Gregorio and Jansen*, 2000] developed by the Food and Agricultural Organization and contains 27 land cover classes.

[18] For an updated representation of land surface, GLC2000 was thus used in these experiments, replacing the default OGE data set. In order to be able to use the biophysical parameters adopted from the Biosphere-Atmosphere Transfer Scheme (BATS) [*Dickinson et al.*, 1986], GLC2000 classes were cross-referenced (Figure 2a) based on the results of multiple assessments [*Torbick et al.*, 2006]. The predominant five nonwater land cover types after cross-referencing are presented in Table 1, with spatial extent percentages and the most important biophysical parameters listed. Combined, the five predominant types comprise 62.13% of the total area, while ocean and inland water combined comprise 12.27%. The largest inland water body in this area is Lake Victoria in the center of the model domain (Figure 2a). In the default LEAF-2 methodology, the original 1 km land cover data is sampled to reduce the demand on computing resources used to initialize the model. Only one pixel's value, for example, is taken from a 5×5 pixel block for a configuration of a 50 km horizontal spacing. As a result, details of the input land cover are lost. In this study, detailed land cover input is needed, and therefore the sampling strategy was modified to take every 1 km land cover pixel in a grid cell.

2.3. Land Cover Accuracy

[19] Land cover accuracy is commonly defined as the degree to which the derived classification agrees with reality [*Foody*, 2002]. Here, classification error at the1 km level was simulated as a random difference from GLC2000 (Figure 2a), the initial baseline land cover which was assumed to be 100% accurate. Specifically, random locations in the 1 km GLC2000 were selected, and the original land cover type at each of these selected locations was replaced by a type randomly chosen from the five predominant types (Table 1). Only land cover types could be chosen to be randomly altered since in practice it is less likely that water bodies are misclassified. The five predominant land classes were chosen, because it is reasonable to assume they have more chance to be misclassified than less abundant classes.

[20] Classification errors with magnitudes ranging from 5% to 50% at 5% intervals were generated. The magnitude of error was determined by the proportion of converted pixels in the 1 km GLC2000. Fifty percent error was the maximum level tested as it was assumed that most land cover products could reach 50% accuracy levels. These 1 km land covers with degraded classification accuracies were then used to initialize the land surface in RAMS simulations, and the behavior of simulated results was examined.

[21] In Figure 2, 10% (Figure 2c), 30% (Figure 2d), and 50% (Figure 2e) classification errors are presented. For the sake of clarity, only the most predominant patches (see section 2.1 for the concept of patch) in each 50 km RAMS grid cell are illustrated because simulated errors and their gradual increase would be hard to see at a 1 km resolution (Figure 2a). Figure 2b presents the land cover in 50 km resolution, which was assumed to be 100% accurate, with each grid cell showing only its most predominant patch. Figures 2c, 2d, and 2e show those model grid cells with the biggest patches changed following the introduction of random classification errors.

[22] Despite random selection at1 km resolution, the errors do not appear to be distributed randomly over the domain when viewed at 50 km level. Instead, they tend to occur at the transition zones between major types (Figure 2b), where it is likely that two land cover types are approximately equal in frequency within the grid cell. Converting a few pixels may alter which land cover type is the predominant patch. For example, most changes in evergreen broadleaf forests in Figures 2c, 2d, and 2e occur at the edge of the Congo forest. For grid cells with strongly dominant types, such as the Congo forest, random errors are less likely to change the dominance of the biggest patch. Transitions to woodland appear to have a higher frequency than do the other four types (see especially in Figure 2e). This is due to the woodland appearing in a fragmented arrangement (Figure 2a). Similarly, transitions to water as the largest patch show up at the edges of lakes and the ocean, as seen in Figures 2c, 2d, and 2e, although water was not considered in the process of randomization (Table 1).

[23] In each experiment, RAMS was run 11 times, each with different amounts of classification error ranging from zero to 50%. The effect of classification accuracy on simulated regional climate was then examined by comparing the behavior of simulated precipitation within this range of accuracies to determine patterns. Then, patterns of behavior were compared across experiments to investigate the impacts of model parameterizations.

3. Results

3.1. Basic Experiment

[24] In the basic experiment, RAMS was run with the KF convection scheme and without nudging. The performance of RAMS was first assessed by comparing the RAMS' simulated accumulated precipitation for the period March–May 2003 against observed data. In this region, rainfall data from weather stations are scarce with extremely low spatial and temporal frequency. A full comparison over the whole domain was therefore not possible. The precipitation

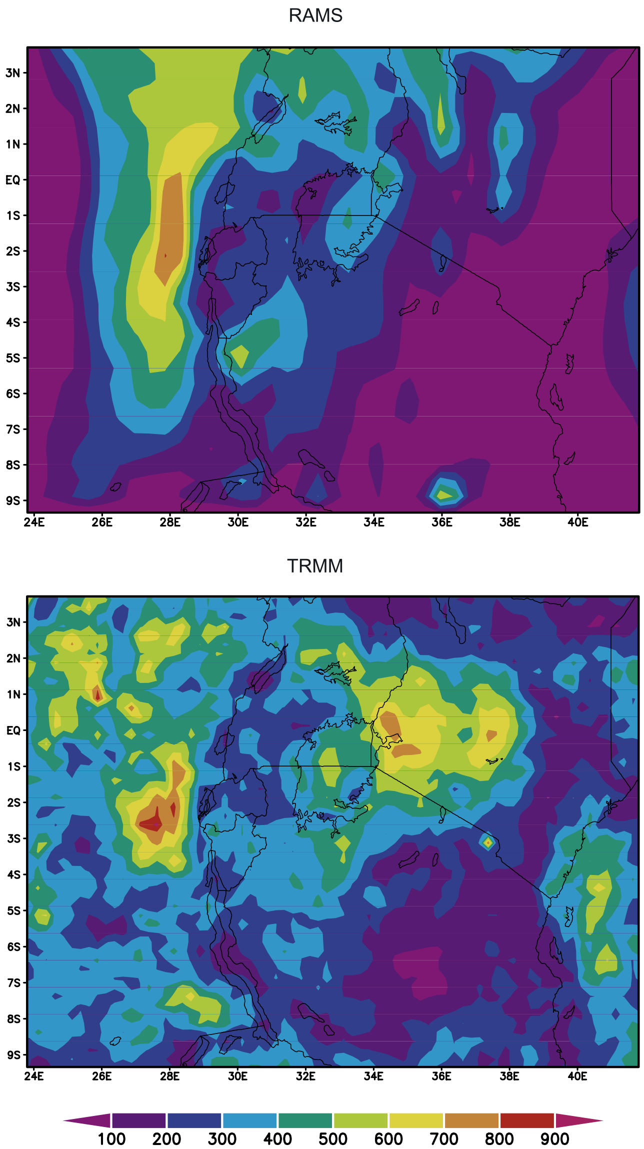

Figure 3. Spatial comparison of simulated accumulated precipitation (mm) in RAMS and that from TRMM.

retrievals from the Tropical Rainfall Measuring Mission (TRMM) satellite were thus used. TRMM is a joint satellite between NASA and the Japan Aerospace Exploration Agency (JAXA), launched in November 1997 [*Simpson et al.*, 1988]. Its primary mission is to measure precipitation in the tropics, using both active and passive microwave instruments. This study used TRMM 3B42 version 6 data products which have 3-hour temporal resolution and $0.25^\circ \times 0.25^\circ$ spatial resolution. Data plots can be generated directly online at http://lake.nascom.nasa.gov/Giovanni/tovas/TRMM_V6.3B42.2.shtml.

[25] Figure 3 shows both the simulated accumulated rainfall from RAMS and observed accumulated rainfall from TRMM. RAMS underestimates precipitation in some areas, especially near the left and right boundaries, which may be due to the effect of boundary nudging. However, it captured some major features, such as over the Congo forest. The spatial distribution of simulated precipitation is fairly similar to observations, especially considering that no attempt was made to "tune" model parameters and that our configuration of RAMS has a lower spatial resolution (50 km versus about 27 km). In Figure 4, precipitation is compared over time. The correlation coefficient is 0.336 for the whole time period, and 0.438 when the spin-up time of the first 20 days is omitted. Fidelity to observation improved over time, and the cessation of the "long rains" (day 77) is well replicated.

[26] The differences in precipitation between the simulation without land cover errors and simulations with errors (5%, 10% ... 45%, 50%) were then examined. For the convenience of discussion, let R00, R05, R10 ... R45, R50 denote these 11 runs and R05-R00, R10-R00 ... R45-R00, R50-R00 denote the differences between runs. R10-R00, R30-R00, and R50-R00 are presented in Figure 5. If classification accuracy does not have any impact on simulated precipitation, then these differences are expected to be close to zero. However, as illustrated in Figure 5, precipitation differences are not minute. The impact on precipitation increases as classification accuracy worsens. It is also noticeable that most of the largest differences occur in the Lake Victoria area, even though errors are scattered across the whole domain (Figure 2).

[27] Although a full investigation of this is beyond the scope of this paper, it is likely that the general spatial pattern of changes in precipitation as shown in Figure 5 is due to the mechanism stated by *Charney et al.* [1977] and followed by other researchers [*Lofgren*, 1995; *Xue*, 1997; *Wang et al.*, 2004]. In this mechanism, change in land surface parameters (e.g., albedo, vegetation fractional cover), alters the energy budget of the coupled surface-atmosphere system. Particularly at low latitudes, reduced heating of the atmosphere, resulting from increased surface albedo, leads to a relative sinking motion and reduced precipitation, while decreased surface albedo and increased atmospheric heating have the opposite effect.

[28] In the domain considered here, the unperturbed GLC2000 land cover has nearly solid evergreen broadleaf

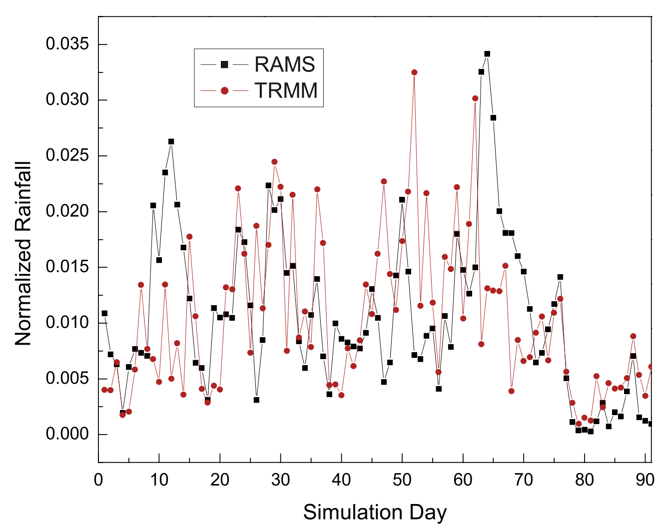

Figure 4. Temporal comparison of simulated cumulative precipitation in RAMS and from TRMM. Domain-averaged daily precipitation is normalized to 1 for the sake of comparison for the study area.

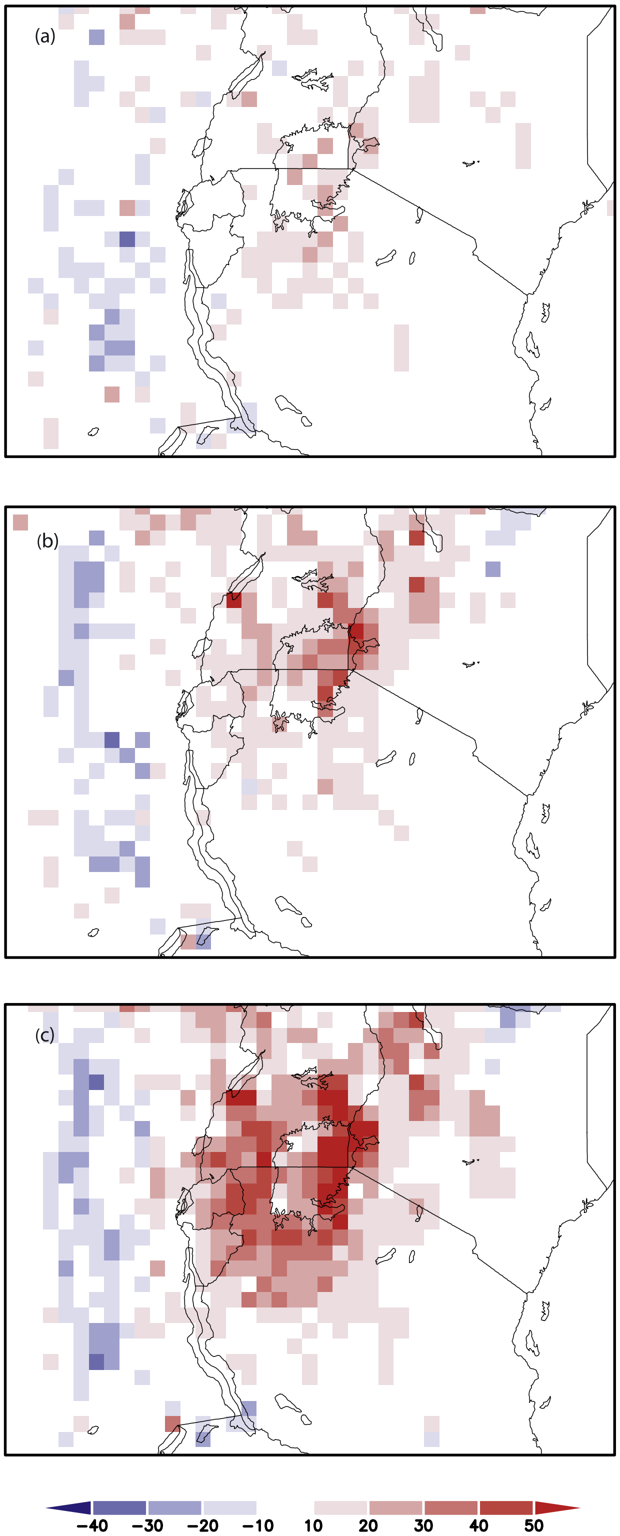

Figure 5. Differences of accumulated precipitation (mm) between simulation without land cover error and simulations with (a) 10% error (R10-R00), (b) 30% error (R30-R00), and (c) 50% error (R50-R00).

forest in the western part of the domain, the class with the lowest surface albedo (Table 1). Thus the insertion of random errors into the land cover will necessarily increase the surface albedo, resulting in reduced precipitation in this area. Conversely, the region surrounding Lake Victoria is initially dominated by the crop/mixed farming class, which has the highest surface albedo of any of the classes used in the random processes, so the imposition of random errors reduces the surface albedo in this region. Combined with the ready access to water evaporating from Lake Victoria itself, this can lead to an increase in precipitation. As shown by *Lofgren* [1995], the heating of the atmosphere near Lake Victoria due to reduced surface albedo and the changes of other parameters is likely compounded by release of latent heat of condensation associated with the increased precipitation.

[29] Three measures were then utilized to depict the precipitation differences between runs (Figure 5). The first measure is the maximum absolute difference (both positive and negative), which highlights only one hot spot. It represents the largest possible difference caused by land cover errors, but it does not give information on the overall differences. The other two measures used are the mean absolute difference and the standard deviation calculated over the whole domain. They characterize the overall magnitude and variation of the difference. As shown in Figure 5, maximum absolute differences for R10-R00, R30-R00, and R50-R00 are 30.6 mm, 56.7 mm, and 84.4 mm; mean absolute differences are 4.6 mm, 6.7 mm, and 10.5 mm; and standard deviations are 6.7 mm, 9.5 mm, and 14.7 mm. The three measures all indicate an increase in precipitation difference as land cover accuracy decreases.

[30] These three measures can evaluate precipitation differences against a range of classification errors (5% to 50%). For the basic experiment, the black lines in Figure 6 show the behavior of precipitation difference for this range of classification errors by illustrating the maximum and mean absolute difference and the standard deviation. In Figure 6a, the maximum absolute difference from the basic experiment increases from 34.8 mm for 5% error to 84.4 mm for 50% error. In Figure 6b, the mean absolute difference increases from 5.5 mm to 10.5 mm. Also, in Figure 6c, standard deviation increases from 7.8 mm to 14.7 mm. From these three plots, it is evident that precipitation differences increase with an increase in land cover errors in RAMS. Importantly, when the errors are less than 20%, the plots are relatively flat, and when errors are larger than 20%, the differences increase sharply. This indicates that a classification error of less than 20% has little effect on the simulated precipitation in this particular experiment. The accuracy target of 85% commonly specified in the land cover production community can meet the requirements of regional climate modeling. If the land cover accuracy is less than 80%, however, its effect on climate simulation and propagation of uncertainty should be examined.

[31] In the basic experiment results shown in Figure 6, the level area below 20% errors has nonzero differences. This is especially obvious for 5% error level. Adding this small amount of classification error causes some precipitation differences. These nonzero differences might be due to a random noise. Above the 20% threshold, the signal rises above the noise. It is noticeable that there is a slight leveling

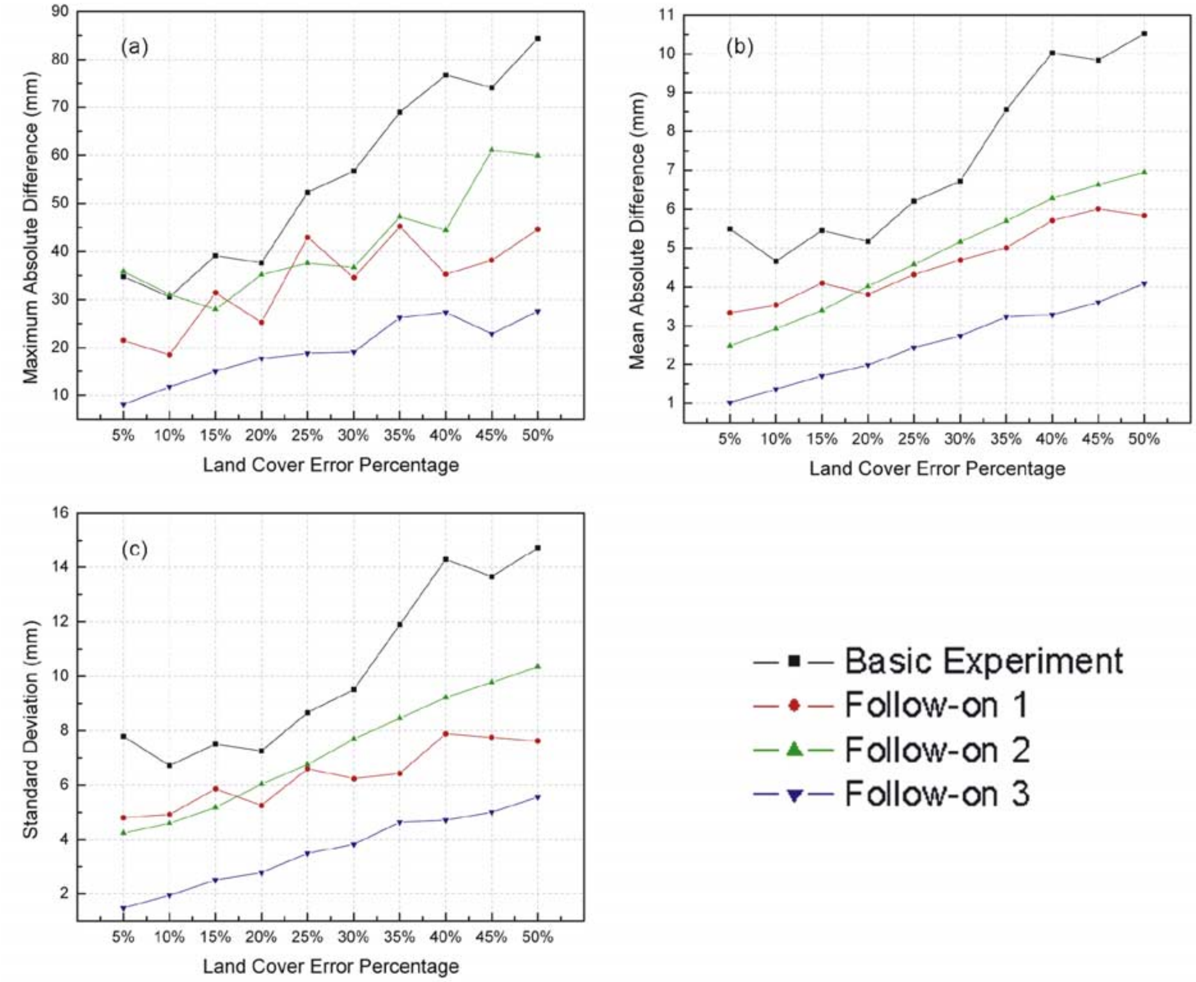

Figure 6. (a) Maximum absolute differences, (b) mean absolute differences, and (c) standard deviations of precipitation from basic experiment (Kain-Fritsch), follow-on 1 (Kuo), follow-on 2 (Kain-Fritsch with interior nudging), and follow-on 3 (Kuo with interior nudging).

off of the differences above the 40% level, which might be due to a saturation effect of classification errors.

3.2. Follow-On Experiments

[32] To test the effect of model parameterizations on atmospheric response to land cover accuracy, internal nudging and a different convection scheme were investigated. A different convection scheme may dramatically change the surface energy and moisture budget and hence surface feedback to the atmosphere. The KF convection scheme, which was used in the basic experiment, is known to produce more precipitation than the Kuo scheme, especially in areas of steep terrain [*Castro et al.*, 2002, 2005]. The nudging is used to relax the model solution toward the input reanalysis data continuously at each time step by adding artificial tendency terms (based on the difference between the two states) to the prognostic equations. With interior nudging, the surface boundary conditions tend to have weaker control on the vertical motion and distribution of precipitation, compared to no interior nudging [*Weaver et al.*, 2002; *Castro et al.*, 2005]. Therefore both convection scheme and interior nudging may influence the effect of land cover accuracy on simulated precipitation in RAMS. Other model aspects can also modify the influence of surface forcing on simulated precipitation; however, nudging and convection schemes are often used for such evaluations [e.g., *Weaver et al.*, 2002; *Castro et al.*, 2005].

[33] In the basic experiment described above, the KF convection scheme was used with no interior nudging, which allowed the model to have a stronger response to surface boundary forcing. In the follow-on experiment 1, the Kuo scheme was used with no interior nudging; In the follow-on experiment 2, the KF scheme was used with interior nudging applied; Also, in the follow-on experiment 3, the Kuo scheme was used together with interior nudging. When interior nudging was used, the timescale was set to 1 day, which is larger than that specified in the RAMS User Guide [*Castro et al.*, 2005]. In each of these three follow-on experiments, RAMS was run 11 times, each with a different amount of classification error ranging from zero to 50%, similar to the basic experiment.

[34] In Figure 7, accumulated precipitation is presented for the basic experiment and the three follow-on experiments, all with no classification error. As expected, the Kuo

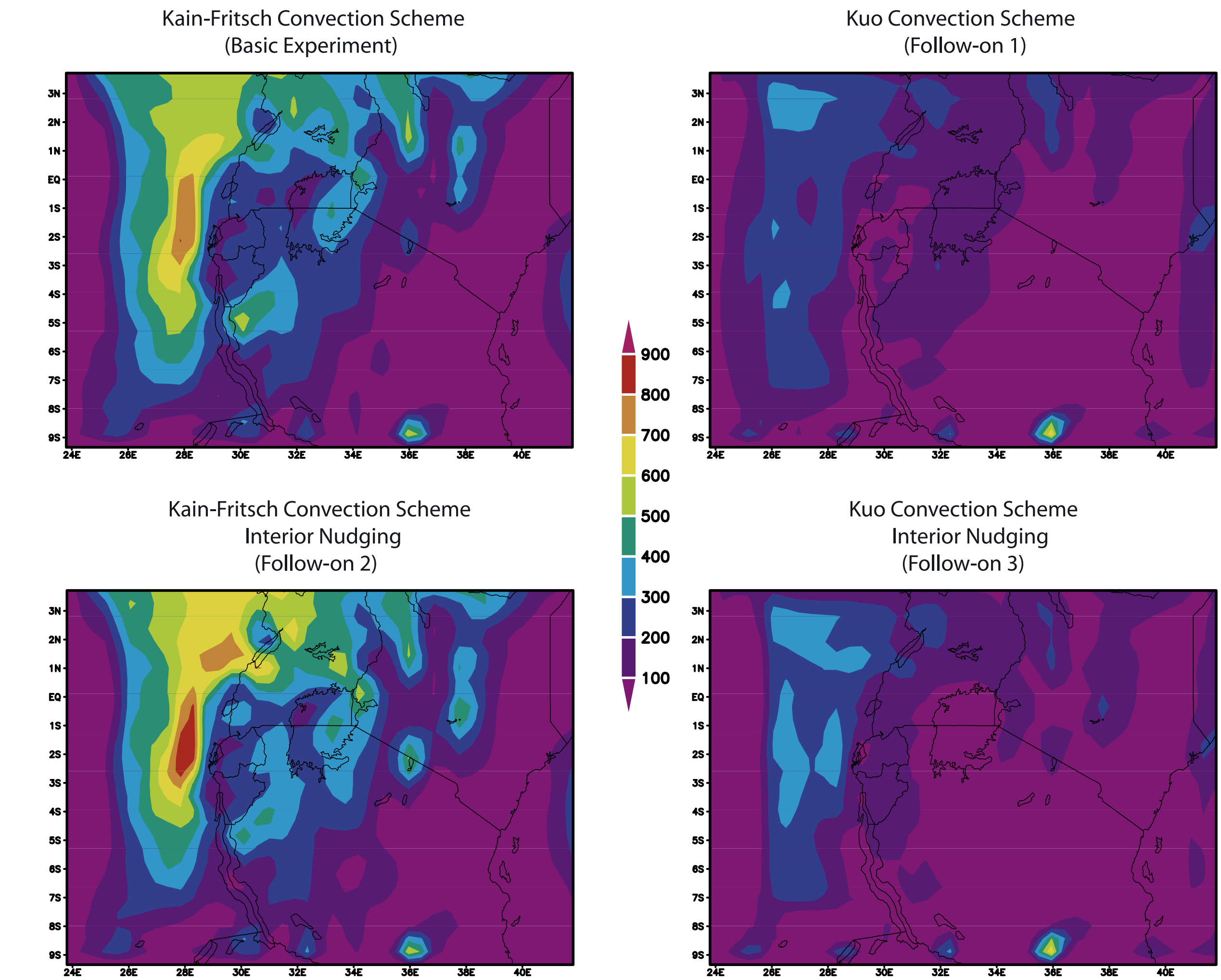

Figure 7. Simulated accumulated precipitation (mm) with different model parameterizations. Results from runs without land cover error are presented.

scheme produces much less precipitation over the whole domain. The major peak over Congo forest, which is seen in experiments with the KF scheme and satellite observations (Figure 3), is not shown clearly in experiments with the Kuo scheme. There is not much difference between these two schemes over dry areas, where both schemes tend to underestimate the precipitation. The interior nudging seems to have little effect on the accumulated precipitation.

[35] In each follow-on experiment, precipitation differences between simulations with and without classification errors were then investigated by examining the maximum and mean absolute differences and the standard deviation as in the basic experiment. In Figure 6, the behaviors of these three measures against a range of classification errors are presented for both the basic experiment and the three follow-on experiments. Precipitation in the follow-on experiments is much less sensitive to classification errors, especially when the Kuo scheme was used. With both convection schemes, interior nudging tends to reduce this sensitivity. Interestingly, standard deviation plots for interior nudging are very close to straight lines. This may be due to the effect of interior nudging reducing the strength of small-scale variability, which has also been reported in other studies [e.g., *Weaver et al.*, 2002].

4. Discussion

[36] In RAMS, each land cover type is represented by a suite of biophysical variables: albedo, leaf area index (LAI), fractional vegetation cover, etc. These biophysical variables determine energy and moisture exchange between the land surface and overlying atmosphere. Thus the effect of land cover classification accuracy on simulated precipitation is ultimately controlled by the changes in the biophysical variables. Therefore the effect of classification accuracy relies on how the surface scheme (LEAF-2 in this study) defines these biophysical variables for each type. As the biophysical parameters of different land cover types become more differentiated, the effect observed in previous sections will be more pronounced. In the hypothetical case when all land covers have exactly the same biophysical characteristics, classification accuracy will not have any effect on simulated precipitation.

[37] In Figure 8, the default RAMS LAI (with the incorporation of the GLC2000 land cover) is compared to

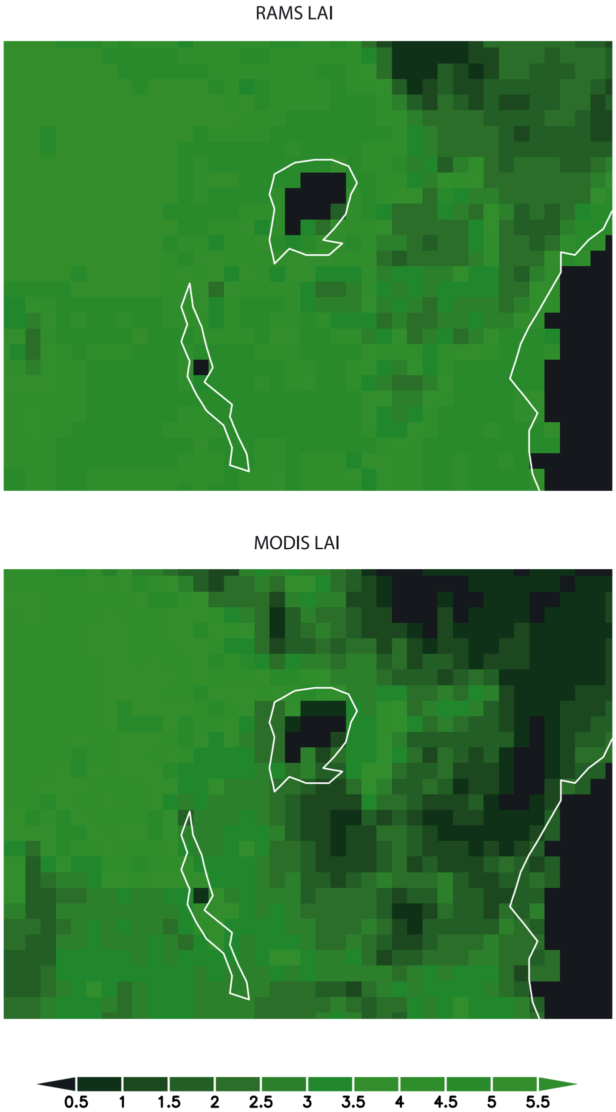

Figure 8. Built-in LAI from RAMS and observed LAI from MODIS, May 2003.

the satellite observed LAI product by MODIS [*Myneni et al.*, 2002] for May 2003. One kilometer MODIS LAI was resampled to 50 km resolution to permit the comparison. It is evident that the LAI in RAMS is unrealistically uniform over most of the domain with several regions poorly represented. Similar patterns are evident in March and April 2003 (not shown). Other biophysical parameters in RAMS version 4.4, such as albedo and fractional vegetation cover, may also have this characteristic of being overhomogeneous since they are defined by simple mathematical functions. Therefore it is reasonable to expect that the impact of classification accuracy on simulated precipitation might be even greater than described in this study.

[38] As shown in the previous sections, land cover accuracy lower than 80% can substantially affect simulated precipitation, especially when the surface has a greater control of the atmosphere. This effect becomes stronger as the accuracy decreases. Although an 85% accuracy target has already been recommended for land cover production, in reality this target is rarely obtained [*Trodd*, 1995]. For example, the IGBP Discover Land Cover product, a land cover layer from GLCC with global coverage, has an overall accuracy of 66.9%, which is comfortably lower than the specified target [*Scepan*, 1999]. Another layer of GLCC, OGE, which is the default land cover data set in RAMS, does not come with an accuracy estimate. Global accuracy for newly developed MODIS Land Cover product (V003) is stated to be approximately 70–80% (http://geography.bu.edu/landcover/userguidelc/consistent.htm). When these global land cover products are used for a specific region, such as East Africa, the accuracy levels can be much lower than the global accuracy. Therefore caution is needed when using global land cover products at regional to local levels. It should also be mentioned that global land cover products are usually developed for land cover identification or other general use. In order to be used in SVAT schemes in climate models, they often need to be cross-referenced, which can add additional uncertainties.

[39] These global products, however, have their advantages. The importance of classification accuracy is well recognized by producers. Quantitative evaluation is therefore conducted to provide guidelines for users. Many land cover data sets employed in climate modeling studies do not come with accuracy information. This is especially true for historically reconstructed and future projected land cover data sets that are often employed to examine the impact of human activities on climate. Historical land covers are usually derived from existing maps and other indirect evidence, while future projected land covers are often developed from spatial models that simulate how changes in land use are likely to affect land cover. There are simply not many options for accuracy assessment of these types of land cover data sets. Historical and future land cover data sets are usually used to simulate time periods that are decades or even centuries long, much longer than the 3 months simulated in this study. The impact of land cover accuracy may well increase over these longer time frames. Uncertainties in those input land cover data sets may cause great uncertainties in the output in climate models.

[40] There are aspects in this work that can be further explored. One is the strategy that was used to simulate classification errors. It was assumed that classification errors occur randomly over space. In reality, they are more likely to occur in areas with greater land surface heterogeneity and not in homogeneous landscapes such as the Congo forest. Also, the original land cover types were replaced by random types from the five predominant types without considering the biophysical similarities between types. Land cover types with similar physical appearances or similar spectral features in satellite images are more likely to be misclassified.

[41] A second aspect relates to the configuration of RAMS. Factors such as horizontal grid spacing and multiple nested grids may influence the effect observed in this paper. The mosaic method of accounting for subgrid variability in land cover does not take into account certain factors. Notably, latent, sensible, and radiative heat fluxes will be dependent on the land cover and on the characteristics of the air in the planetary boundary layer. The boundary layer atmospheric characteristics are likely to be spatially correlated with the land cover, but the mosaic approach does not

account for this and thus will miss the nonlinear effects on fluxes. The situation is further complicated by subgrid mesoscale circulations that can be forced by land cover heterogeneity [e.g., *Weaver and Avissar*, 2001]. These factors can be sensitive to the scale over which land cover is altered in addition to the model grid spacing. Further investigations considering these factors are needed.

5. Summary

[42] Human activities have substantially modified the Earth's surface in the past and will continue to do so in the future. The impact of human activities such as land cover change on regional and the global climate can be studied using climate modeling techniques. Land cover data sets, often derived from remote sensing images, are widely used in land surface schemes in climate models to describe the physical surface conditions. These data sets are not perfect, and their value is a function of classification accuracy. In the land cover production process quantitative accuracy assessment has almost become a required procedure. However, the accuracy of land cover data sets and its impact on simulated climate have largely been ignored in climate modeling research.

[43] In this paper, the Regional Atmospheric Modeling System was utilized to study the impact of land cover accuracy on simulated precipitation for the East Africa region. Classification errors were simulated as random alterations to the land cover data set used in this study, GLC2000. The behavior of simulated accumulated precipitation over a 3 month period was then examined over a range of land cover errors (zero to 50%). It was found that, when the surface boundary had greater control on overlaying atmosphere, land cover accuracy under 80% had a strong effect on simulated precipitation. As land cover accuracy worsened, this effect became stronger. This effect was shown to be moderated by model parameterizations such as convection schemes and interior nudging, which affected the strength of the control that the surface exerts on the atmosphere. When the Kuo convection scheme was used, RAMS severely underestimated the precipitation over the entire domain, and the land cover accuracy had little effect on simulated precipitation. With interior nudging activated, the effect of land cover accuracy also decreased, even though the overall magnitude of precipitation was affected only slightly.

[44] On the basis of the results of this study, it can be concluded that land cover data sets can meet general needs in climate modeling research if the commonly recommended 85% accuracy target is obtained. In reality, however, this is usually not the case. The reliability of land cover data sets needs to be examined in climate modeling research, especially those using historically reconstructed or future projected land covers for long-term simulations.

[45] **Acknowledgments.** Part of this research was funded by the NASA grant NNG05GD49G and the National Science Foundation Biocomplexity of Coupled Human and Natural Systems Program award BCS 0308420. This is GLERL contribution 1406.

References

Brown, J. F., T. R. Loveland, D. O. Ohlen, and Z. Zhu (1999), The global land-cover characteristics database: The users' perspective, *Photogramm. Eng. Remote Sens.*, *65*, 1069–1074.

Castro, C. L., W. Y. Y. Cheng, A. B. Beltrán, C. H. Marshall Jr., R. A. Pielke Sr., and W. R. Cotton (2002), The incorporation of the Kain-Fritsch cumulus parameterization scheme in RAMS with a terrain-adjusted trigger function, paper presented at Fifth RAMS Users and Related Applications Workshop, ATMET Inc., Santorini, Greece.

Castro, C. L., R. A. Pielke Sr., and G. Leoncini (2005), Dynamical downscaling: Assessment of value retained and added using the Regional Atmospheric Modeling System (RAMS), *J. Geophys. Res.*, *110*, D05108, doi:10.1029/2004JD004721.

Charney, J., W. J. Quirk, S.-H. Chow, and J. Kornfield (1977), A comparative study of the effects of albedo change on drought in semi-arid regions, *J. Atmos. Sci.*, *34*, 1366–1385.

Chase, T. N., R. A. Pielke Sr., T. G. F. Kittel, J. S. Baron, and T. J. Stohlgren (1999), Potential impacts on Colorado Rocky Mountain weather due to land use changes on the adjacent Great Plains, *J. Geophys. Res.*, *104*(D14), 16,673–16,690.

Chase, T. N., R. A. Pielke Sr., T. G. F. Kittel, R. Nemani, and S. W. Running (2000), Simulated impacts of historical land cover changes on global climate in northern winter, *Clim. Dyn.*, *16*, 93–105.

Chen, C., and W. R. Cotton (1983), A one-dimensional simulation of the stratocumulus-capped mixed layer, *Bound Layer Meteorol.*, *25*, 289–321.

Cihlar, J. (2000), Land cover mapping of large areas from satellites: Status and research priorities, *Int. J. Remote Sens.*, *21*, 1093–1114.

Cotton, W. R., et al. (2003), RAMS 2001: Current status and future directions, *Meteorol. Atmos. Phys.*, *82*, 5–29.

DeFries, R. S., L. Bounoua, and G. J. Collatz (2002), Human modification of the landscape and surface climate in the next fifty years, *Global Change Biol.*, *8*, 438–458.

Dickinson, R. E., A. Henderson-Sellers, P. J. Kennedy, and M. F. Wilson (1986), Biosphere-atmosphere transfer scheme for the NCAR community climate model, *NCAR Tech. Note NCAR/TN-275+STR*, Natl. Cent. for Atmos. Res., Boulder, Colo.

Di Gregorio, A., and L. J. M. Jansen (2000), Land cover classification system (LCCS): Classification concepts and user manual, Food and Agric. Organ., U. N., Rome.

Feddema, J. J., K. W. Oleson, G. B. Bonan, L. O. Mearns, L. E. Buja, G. A. Meehl, and W. M. Washington (2005), The importance of land-cover change in simulating future climates, *Science*, *310*, 1674–1678.

Foody, G. M. (2002), Status of land cover classification accuracy assessment, *Remote Sens. Environ.*, *80*, 185–201.

Friedl, M. A., et al. (2002), Global land cover mapping from MODIS: Algorithms and early results, *Remote Sens. Environ.*, *83*, 287–302.

Ge, J., J. Qi, N. Torbick, J. M. Olson, and D. P. Lusch (2007), Biophysical evaluation of four land covers for land-climate interaction modeling in East Africa, *Remote Sens. Environ.*, in press.

Giorgi, F., and L. O. Mearns (1999), Introduction to special section: Regional climate modeling revisited, *J. Geophys Res.*, *104*, 6335–6352.

Houghton, R. A., J. L. Hackler, and K. T. Lawrence (1999), The U.S. carbon budget: Contributions from land-use change, *Science*, *285*, 574–578.

International Geosphere-Biosphere Programme (1990), The International Geosphere-Biosphere Programme: A study of global change- the initial core projects, *IGBP Rep. 12*, Stockholm.

Jacob, D., and R. Podzun (1997), Sensitivity studies with the regional climate model REMO, *Meteorol. Atmos. Phys.*, *63*, 119–129.

Kain, J. S., and J. M. Fritsch (1993), Convective parameterization for mesoscale models: The Kain-Fritsch scheme, in *The Representation of Cumulus Convection in Numerical Models*, *Meteorol. Monogr.*, vol. 24, edited by K. A. Emanuel and D. J. Raymond, pp. 165–170, Am. Meteorol. Soc., Boston, Mass.

Kalnay, E., et al. (1996), The NCEP/NCAR 40-year reanalysis project, *Bull. Am. Meteorol. Soc.*, *77*, 437–471.

Kuo, H. L. (1974), Further studies of the parameterization of the influence of cumulus convection on large-scale flow, *J. Atmos. Sci.*, *31*, 1232–1240.

Lambin, E. F., et al. (1999), Land-use and land-cover change (LUCC): Implementation strategy, *IGBP Rep. 48*, Int. Geosphere-Biosphere Programme, Stockholm.

Lee, T. J. (1992), The impact of vegetation on the atmospheric boundary layer and convective storms, *Atmos. Sci. Pap. 509*, Colo. State Univ., Fort Collins, Colo.

Lofgren, B. M. (1995), Sensitivity of land-ocean circulations, precipitation, and soil moisture to perturbed land surface albedo, *J. Clim.*, *8*, 2521–2542.

Loveland, T. R., B. C. Reed, J. F. Brown, D. O. Ohlen, Z. Zhu, L. Yang, and J. W. Merchant (2000), Development of a global land cover characteristics database and IGBP DISCover from 1 km AVHRR data, *Int. J. Remote Sens.*, *21*, 1303–1330.

Matthews, E. (1983), Global vegetation and land use: New high resolution data bases for climate studies, *J. Clim. Appl. Meteorol.*, *22*, 474–487.

Mayaux, P., E. Bartholomé, S. Fritz, and A. Belward (2004), A new land-cover map of Africa for the year 2000, *J. Biogeogr.*, *31*, 861–877.
Mellor, G. L., and T. Yamada (1982), Development of a turbulence closure model for geophysical fluid problems, *Rev. Geophys.*, *20*, 851–875.
Myneni, R. B., et al. (2002), Global products of vegetation leaf area and fraction absorbed PAR from year one of MODIS data, *Remote Sens. Environ.*, *83*, 214–231.
Olson, J. S., J. A. Watts, and L. J. Allison (1983), Carbon in live vegetation of major world ecosystems, *Rep. ORNL-5862*, Oak Ridge Natl. Lab., Oak Ridge, Tenn.
Pielke, R. A., Sr. (2001), Influence of the spatial distribution of vegetation and soils on the prediction of cumulus convective rainfall, *Rev. Geophys.*, *39*, 151–177.
Pielke, R. A., Sr., et al. (1992), A comprehensive meteorological modeling system-RAMS, *Meteorol. Atmos. Phys.*, *49*, 69–91.
Pielke, R. A., Sr., R. L. Walko, L. T. Steyaert, P. L. Vidale, G. E. Liston, W. A. Lyons, and T. N. Chase (1999), The influence of anthropogenic landscape changes on weather in south Florida, *Mon. Weather Rev.*, *127*, 1663–1673.
Reynolds, R. W., and T. M. Smith (1994), Improved global sea surface temperature analyses using optimum interpolation, *J. Clim.*, *7*, 929–948.
Scepan, J. (1999), Thematic validation of high-resolution global land-cover data sets, *Photogramm. Eng. Remote Sens.*, *65*, 1051–1060.
Sellers, P. J., Y. Mintz, Y. C. Sud, and A. Dalcher (1986), A simple biosphere model (SiB) for use within general circulation models, *J. Atmos. Sci.*, *43*, 505–531.
Sellers, P. J., D. A. Randall, G. J. Collatz, J. A. Berry, C. B. Field, D. A. Dazlich, C. Zhang, G. D. Collelo, and L. Bounoua (1996a), A revised land surface parameterization (SiB2) for atmospheric GCMs. part 1: Model formulation, *J. Clim.*, *9*, 676–705.
Sellers, P. J., S. O. Los, C. J. Tucker, C. O. Justice, D. A. Dazlich, G. J. Collatz, and D. A. Randall (1996b), A revised land surface parameterization (SiB2) for atmospheric GCMs. part 2: The generation of global fields of terrestrial biophysical parameters from satellite data, *J. Clim.*, *9*, 706–737.
Simpson, J., R. F. Adler, and G. R. North (1988), A proposed tropical rainfall measuring mission (TRMM) satellite, *Bull. Am. Meteorol. Soc.*, *69*, 278–295.
Smagorinsky, J. (1963), General circulation experiments with the primitive equations. part I: The basic experiment, *Mon. Weather Rev.*, *91*, 99–164.
Taylor, C., E. F. Lambin, N. Stephenne, R. Harding, and R. Essery (2002), The influence of land-use change on climate in the Sahel, *J. Clim.*, *15*, 3615–3629.
Thomlinson, J. R., P. V. Bolstad, and W. B. Cohen (1999), Coordinating methodologies for scaling landcover classifications from site-specific to global: Steps toward validating global map products, *Remote Sens. Environ.*, *70*, 16–28.
Torbick, N., D. P. Lusch, J. Qi, N. Moore, J. M. Olson, and J. Ge (2006), Developing land use/land cover parameterization for climate-land modeling in East Africa, *Int. J. Remote Sens.*, *27*, 4227–4244.
Tremback, C. J., and R. Kessler (1985), A surface temperature and moisture parameterization for use in mesoscale models, paper presented at Seventh Conference on Numerical Weather Prediction, Am. Meteorol. Soc., Montreal, Ont., Canada.
Trodd, N. M. (1995), Uncertainty in land cover mapping for modeling land cover change, paper presented at RSS95 Remote Sensing in Action, Remote Sens. Soc., Southampton, U.K.
Walko, R. L., et al. (2000), Coupled atmosphere-biophysics-hydrology models for environmental modeling, *J. Appl. Meteorol.*, *39*, 931–944.
Wang, G., E. A. B. Eltahir, J. A. Foley, D. Pollard, and S. Levis (2004), Decadal variability of rainfall in the Sahel: Results from the coupled GENESIS-IBIS atmosphere-biosphere model, *Clim. Dyn.*, *22*, 625–637.
Watson, R. T., I. R. Noble, B. Bolin, N. H. Ravindranath, D. J. Verardo, and D. J. Dokken (2000), Land use, land use change, and forestry, *IPCC Special Rep.*, Intergov. Panel on Clim. Change, Geneva, Switzerland.
Weaver, C. P., and R. Avissar (2001), Atmospheric disturbances caused by human modification of the landscape, *Bull. Am. Meteorol. Soc.*, *82*, 269–281.
Weaver, C. P., S. B. Roy, and R. Avissar (2002), Sensitivity of simulated mesoscale atmospheric circulations resulting from heterogeneity to aspects of model configuration, *J. Geophys. Res.*, *107*(D20), 8041, doi:10.1029/2001JD000376.
Xue, Y. (1997), Biosphere feedback on regional climate in tropical north Africa, *Q. J. R. Meteorol. Soc.*, *123*, 1483–1515.

J. Ge, N. Moore, J. Qi, and N. Torbick, Department of Geography and Center for Global Change and Earth Observations, Michigan State University, 116 Geography Building, East Lansing, MI 48824-1115, USA. (gejianju@msu.edu)

B. M. Lofgren, NOAA Great Lakes Environmental Research Laboratory, 2205 Commonwealth Boulevard, Ann Arbor, MI 48105-2945, USA.

J. M. Olson, Department of Geography, Michigan State University, 116 Geography Building, East Lansing, MI 48824-1115, USA.